SOLAR WIND COMPRESSION OF THE MAGNETIC ANOMALY AT REINER GAMMA AND POTENTIAL WEATHERING PATTERNS OBSERVED IN THE ULTRAVIOLET. C.D. Waller[1], J.T.S. Cahill[1], K.D. Retherford[2,3], A.R. Hendrix[4], [1]Johns Hopkins APL, Laurel, MD (email: Dany.Waller@jhuapl.edu), [2]SwRI, San Antonio, TX, [3]UT, San Antonio, TX, [4]PSI, Tucson, AZ

Introduction: While the Moon presently lacks a global, internally-generated magnetic field, the lunar crust contains many regions of localized magnetization known as magnetic anomalies, which are strongly correlated with lunar swirls [1,2]. Swirls are a type of lunar surface feature characterized by sinuous patterns of atypical reflectance that show spatial similarities with their associated magnetic anomalies. Among other theories, swirls are hypothesized to be the result of magnetic shielding from solar wind exposure [3,4]. To explore the formation and possible origin of these swirls, Reiner Gamma was selected by NASA to visit in the next ~2.5 years by the Lunar Vertex (LVx) mission [5].

In preparation for the launch of LVx in April of 2024, potential solar wind interactions with the magnetic anomaly associated with Reiner Gamma have been modeled based upon orbital magnetic data and examined relative to ultraviolet (UV) datasets. UV wavelengths are sensitive to the effects of solar wind weathering, which is caused in part by sputtering and implantation of solar wind ions and electrons [6,7]. These charged particles are influenced by electromagnetic forces like the magnetic anomaly associated with Reiner Gamma. The Lorentz force deflects charged particles incident at normal angles upon magnetic field lines. Thus, understanding the field morphology of swirl-associated magnetic anomalies is crucial to determining if solar wind standoff is possible [8]. The surface field intensity and directionality are examined relative to UV datasets utilizing cross-sectional spatial profiles to explore potential patterns suggesting solar wind weathering disruption.

Methods: Here a three-dimensional magnetic field model was created from Lunar Prospector fluxgate magnetometer (LPMAG) data, starting from an average orbital altitude of 30 kilometers and downward continued to the lunar surface [9]. Note that while the inversion techniques are sound, they may provide somewhat incomplete views of crustal magnetic field structure and intensity due to attenuation of signal as a function of distance from the source. Despite this imperfection, these results are still crucial for field models approaching the surface as the near-surface geometry influences potential solar wind deflection via the Lorentz force.

Similar to Earth's magnetosphere, lunar magnetic anomalies are compressed by the dynamic pressure of incident solar wind, and lunar "mini-magnetospheres" are established when the magnetic pressure of the anomaly is equal to or greater than the solar wind pressure [10,11,12]. Given the data selection criteria of [9], which used orbits with minimal solar wind exposure for inversion, the 3D LPMAG magnetic field is theoretically uncompressed and represents the potential mini-magnetosphere structure under low solar wind pressure.

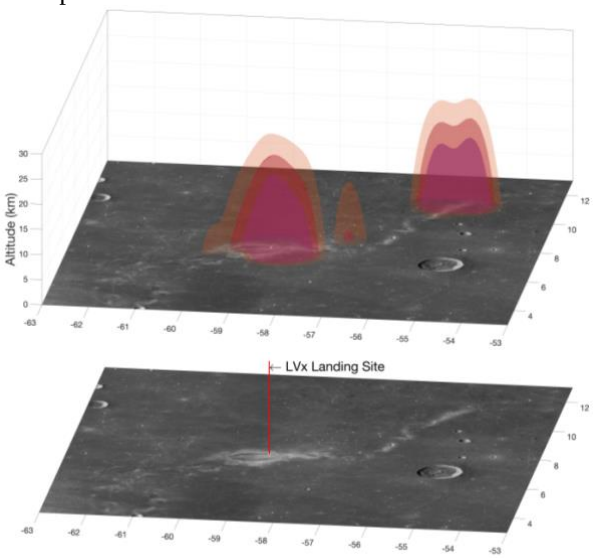

Figure 1: *The compressed magnetic anomaly at Reiner Gamma that LVx will encounter. Model data are projected onto a 415 nm base map from the LROC WAC. The anomaly is divided into three thresholds of average magnetic intensity at 50/70/90 nT. The white dot represents the current LVx landing site, indicated by a red arrow on the bottom.*

A compressed magnetic model (**Fig. 1**) was constructed by reducing the 3D LPMAG model based on theoretical "standoff" boundaries under varying solar wind conditions.

For a thorough understanding of the Reiner Gamma magnetic anomaly through a lunar orbit, both compressed (high solar wind pressure – unshielded sun-facing solar wind pressure) and uncompressed (low solar wind pressure – 1/500 of sun-facing solar wind pressure) models were computed and projected onto UV base maps from the Lunar Reconnaissance Orbiter Camera (LROC) Wide Angle Camera (WAC) and Lyman-Alpha Mapping Project (LAMP) spectrograph. Spatial profiles of these maps were sampled in areas of the anomaly that the model

predicted to be compressed by solar wind, and compared to profiles in areas that were predicted to be reduced but not completely compressed.

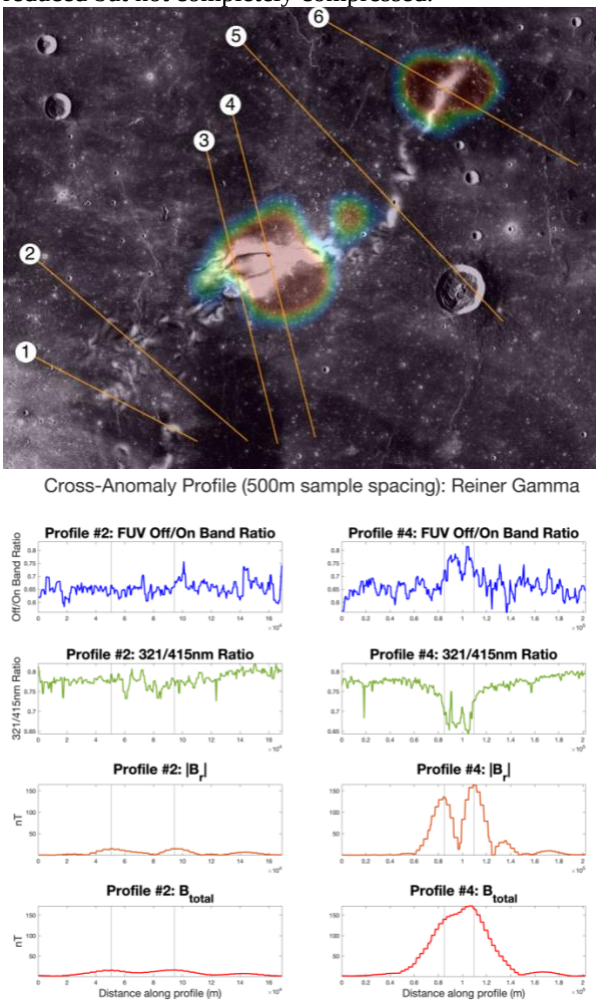

Figure 2: *Select spatial profiles (#2 and 4) across Reiner Gamma sampling LAMP FUV Off/On Band Ratio and LROC WAC 321/415 nm Ratio, and LPMAG $|B_r|$ and B_{total}. Vertical lines on each profile show the peak of the radial component contribution ratio, $|B_r|/ B_{total}$. LVx landing site denoted by black dot on Profile #4.*

Results: In Profile #2, the mini-magnetosphere is compressed to the surface under high pressure solar wind conditions and the regolith seems to experience marginally reduced weathering compared to the relatively unmagnetized background around the swirl in **Figure 2**.

In contrast, sampling across the anomaly at Profile #4 shows a mini-magnetosphere that is sustained during high pressure solar wind conditions, and the highest peaks of the radial field component are spatially close to the inflections of slope in all spectral measurements associated with the edges of the Reiner Gamma anomaly. This agrees with the results of recent studies of energy flux to the surface and follows the Lorentz deflection force theory [13].

Notably in **Figure 2**, there are small inflections in the spectral measurements within the shielded regions of Profile #4 that indicate the swirl may still experience some weathering inside the mini-magnetosphere. This weathering is reduced relative to weathering outside the anomaly and could indicate incomplete standoff due to ion penetration within the mini-magnetosphere, increased solar wind compression during coronal mass ejections, or secondary effects from induced currents and interactions with external magnetic fields. It could also suggest magnetic anomaly structure not currently realized by the surface field model here because, as previously mentioned, inversion techniques cannot fully recover attenuated magnetic signal.

Discussion: This model predicts uneven amounts of solar wind exposure across Reiner Gamma as a result of magnetic anomaly compression by incident solar wind, which is supported by trends observed in near- and far-UV profiles across the areas described above. It also predicts that the LVx lander and rover will observe varying degrees of solar wind compression of the Reiner Gamma magnetic anomaly, and thus may experience varying degrees of radiation during its 2-week mission.

Magnetic anomalies that are completely compressed into the surface may be generating secondary magnetic and electric field interactions, as induced currents are poorly dissipated away into the surrounding regolith. This is subject to variance under temperature via the Wiedemann-Franz Law, and magnetic compression is also dependent on the particle velocity and density and angle of incidence of solar wind.

This also offers a potential explanation for swirls observed in UV that are not immediately apparent in visible and near-infrared wavelengths as described in [14], as time-varying exposure to solar wind may be creating reduced and uneven weathering patterns observable only from certain perspectives and wavelength sensitivities. Further analysis is underway to examine this possibility.

References: [1] D. Blewett et al. (2011) *JGR, 116*, E02002. [2] B. Denevi et al. (2016) *Icarus, 273*, 53. [3] R. Bamford et al. (2016) *Astrophys. J., 830*, 146. [4] J. Deca et al. (2018) *Nat. Commun. Phys., 1*, 12. [5] D. Blewett et al. (2021) *AGU, CII*, P55E–1988. [6] A. Hendrix et al. (2016) *Icarus, 273*, 68. [7] C. Pieters and S. Noble (2016) *JGR: Planets, 121*, 1865. [8] D. Hemingway and I. Garrick-Bethell (2012) *JGR, 117*, E10012. [9] D. Ravat et al. (2020) *JGR: Planets, 125*, e2019JE006187. [10] S. Fatemi et al. (2015) *JGR: Space Physics, 120*, 4719. [11] J. Halekas et al. (2017) *JGR: Space Physics, 122*, 6240. [12] F. Cruz et al. (2017) *Phys. Plasmas, 24*, 022901. [13] J. Deca et al. (2020) *JGR: Planets, 125*, e2019JE006219. [14] J. Cahill et al. (2019) *JGR: Planets, 124*, 294.